Mass scaling laws due to isotopic effects in the energy loss of He^{2+} colliding with H, D, and T

R. Cabrera-Trujillo*
Instituto de Ciencias Físicas, Universidad Nacional Autónoma de México, Ap. Postal 48-3, Cuernavaca, Morelos 62251, Mexico and Quantum Theory Project, Departments of Chemistry and Physics, University of Florida, Gainesville, Florida 32611-8435, USA

J. R. Sabin, Y. Öhrn, and E. Deumens
Quantum Theory Project, Departments of Chemistry and Physics, University of Florida, Gainesville, Florida 32611-8435, USA

N. Stolterfoht
Helmholtz-Zentrum für Materialien und Energie, Glienickerstraße 100, D-14109 Berlin, Germany and Quantum Theory Project, Departments of Chemistry and Physics, University of Florida, Gainesville, Florida 32611-8435, USA

(Received 22 November 2010; published 31 January 2011)

Total, electronic, and nuclear energy loss as well as stopping cross sections are calculated for He^{2+} ions incident on atomic hydrogen, deuterium, and tritium at low to intermediate energies by means of an *ab initio*, nonadiabatic approach for solving the Schrödinger equation incorporating coupled electron and nuclear dynamics. Comparison of this *ab initio* treatment with classical nuclear stopping cross-section formulations obtained from Coulomb and screened potential models, and an *ab initio* theory, allows us to deduce scaling laws that incorporate the different target masses (target isotopic effect). We provide a discussion on the range of validity of the use of classical trajectories. We verify that the nuclear energy loss is a universal function of the center-of-mass (c.m.) scattering angle. The scattering angle in the c.m. system shows a dependence on the projectile charge due to a strong isotopic effect on the charge-transfer cross section. In the case of a Coulombic interaction, that dependence disappears, and leads to a formulation based only on the c.m. collision energy for the nuclear stopping cross section. Due to the small electron capture cross section for He^{2+} on H, D, and T in the low-energy region, it is shown that the effective charge model that assumes neutralization of the projectile does not apply to the energy loss of He^{2+} ions in the calculation of stopping cross sections. Thus, for this system, there is no influence of the charge exchange isotope effect of the target in the nuclear stopping cross section of the projectile. In the electronic energy loss, such an isotopic effect is present through Stueckelberg oscillations, but its contribution is small. Furthermore, the electronic stopping cross section shows a threshold effect that results from the minimum momentum transfer necessary to produce an electronic excitation in the target. Finally, the nuclear stopping cross section has a universal behavior as a function of the c.m. collision energy, and care must be taken when comparing ionic systems stopping cross-section results to those of neutral systems as obtained by effective charge models.

DOI: 10.1103/PhysRevA.83.012715 PACS number(s): 34.50.Bw, 34.10.+x, 34.20.Cf, 34.70.+e

I. INTRODUCTION

When a projectile impinges on a target, it may transfer part of its energy to the target. For atomic targets, the energy transfer is separated into electronic energy loss and nuclear energy loss. The electronic energy loss is projectile kinetic energy absorbed by the target, resulting in electronic excitations and ionization of projectile and target electrons. The nuclear energy loss is projectile kinetic energy transferred to the target nuclei and produces target displacements. By this process it is possible to damage the material, break molecular bonds, kill cellular tissue, and many other processes in materials science, plasma physics, astrophysics, radiotherapy, and dosimetry.

The stopping cross section of the target, which measures the ability of the target to absorb projectile kinetic energy, is defined as [1]

$$S(E_0) = \int \Delta T(\theta, E_0) \frac{d\sigma}{d\Omega}\, d\Omega = 2\pi \int_0^\infty b \Delta T(b, E_0)\, db, \tag{1}$$

where E_0 is the projectile incident energy and $d\sigma/d\Omega$ is the differential cross section for a projectile scattering with an angle θ in the laboratory frame of reference. In a classical treatment of the projectile and target nuclei, the scattering angle can be related to the impact parameter, b, by means of the deflection function. Here ΔT is the kinetic energy loss of the projectile, which may have contributions resulting from electronic excitations of both the projectile and target as well as from charge exchange. The dependence of the nuclear energy loss, ΔT_n, on the projectile and target charge has been studied since the earliest work of Bohr [2]. However, little work exists on the dependence of the nuclear energy loss on target mass. In the work of Ziegler, Biersack, and Littmark [3], there is a detailed study of the classical energy loss of a projectile colliding on an atomic target. They include both the projectile and target mass. However, the interaction between projectile and target is treated through a universal potential between two screened neutral atoms, and no explicit mention of the target isotopic effect is made, that is, a target with the same electronic structure but different nuclei mass (isotope). In this work, we address the problem of energy loss dependence on target mass by studying the energy loss of He^{2+} ions colliding with atomic hydrogen, deuterium, and tritium using

*trujillo@fis.unam.mx

an *ab initio* approach that takes into account the dynamical electronic and nuclear interaction of the system.

He^{2+} ions colliding with atomic hydrogen form the simplest asymmetrical, one-electron system for collision studies. In addition, atomic hydrogen and helium are the most abundant elements in the universe and are fundamental in terrestrial plasma fusion. The main constituent of the solar wind, after protons, are He^{2+} ions, which comprise up to a few percent. When these ions interact with planetary atmospheres, there may be charge exchange resulting in target electronic excited states. Subsequent decay of these states can generate vacuum ultraviolet (VUV) emission, which can be used as a diagnostic tool [4,5]. Projectile ions will also lose kinetic energy in the collision and slow down. The main reaction of auroral ions with the outer parts of the terrestrial atmosphere is with atomic hydrogen [6], with typical interaction energies in the range of 50–2000 eV/amu. In Tokamak fusion plasmas, helium ash is the main product of the deuterium-tritium fusion reaction and constitutes an important ingredient in the dynamics of maintaining the plasma. In the boundary layer of the plasma (sheath), a significant fraction of neutral D and T atoms, which are being desorbed and sputtered from the walls, is available for charge exchange reactions and energy loss processes when colliding with α particles. In dosimetry and radiotherapy, the use of H^+ and He^{2+} ion beams in the treatment of tumors has seen an increase in recent years [7]. Because of its importance in a wide variety of applications, a proper understanding of the dynamics of the interaction between He^{2+} ions and H atoms over a large range of collision energies is necessary.

In spite of the apparent simplicity of this one-electron system, it has provided a deep understanding of the detailed dynamics of ion-atom collisions. Previous studies of the He^{2+} + H system [8–11] have shown that the probability for charge transfer in collisions exhibits sinusoidal oscillations (Stueckelberg oscillations) when plotted as a function of the impact parameter. In particular, we have shown a target isotopic effect on the charge-transfer cross section when He^{2+} collides with deuterium and tritium targets [11–13]. It was found that at collision energies of less than 100 eV/amu, the electron capture cross sections for the target atoms D and T exceed those for H by several orders of magnitude. This finding is attributed to differences in the rotational coupling among the colliding particles at small impact parameters for the different target isotopes. Trajectory effects on excitation and capture processes have been studied before [14], however their importance for isotope effects has only recently been observed [12].

In the present work, we study the energy loss (stopping cross section) of He^{2+} ions colliding with H, D, and T by explicitly coupling electron and nuclear dynamics while solving the time-dependent Schrödinger equation. The important aspect of the present work is the investigation of isotopic effects and scaling laws for the nuclear energy loss of the projectile when time-dependent charge exchange processes are present as a function of impact parameter, the target mass, and projectile velocity. The corresponding isotope effects were found to be significant for the intermediate impact parameters at low collision energies. Thus, we report scaling rules for the energy loss of a projectile colliding on targets with different mass but the same initial electronic structure. Atomic units, $\hbar = e = m_e = 1$, are used in this work unless stated otherwise.

II. ELECTRON-NUCLEAR DYNAMICS

To calculate the energy transfer and excitations during a collision, we simultaneously solve for the electronic and nuclear degrees of freedom in the Schrödinger equation during the collision. We have previously employed such an approach in the study of atomic and molecular collisions, using electron-nuclear dynamics (END) [15].

The time dynamics in END are made at the level of the Lagrangian $L = \langle\psi|i\frac{\partial}{\partial t} - H|\psi\rangle/\langle\psi|\psi\rangle$, with ψ the total system wave function. The principle of least action, $\delta A = \delta\int_{t_1}^{t_2} L dt = 0$, is applied to yield the dynamical equations that approximate the time-dependent Schrödinger equation for the simultaneous coupled dynamics of electrons and nuclei.

The simplest level of the END method uses the system wave function

$$|\psi\rangle = |R, P\rangle|z, R, P\rangle, \tag{2}$$

where the nuclear wave function is given by

$$\langle X|R, P\rangle = \prod_k e^{-\frac{1}{2}(\frac{\mathbf{X}_k-\mathbf{R}_k}{\omega})^2 + i\mathbf{P}_k\cdot(\mathbf{X}_k-\mathbf{R}_k)}. \tag{3}$$

The electronic wave function is written as a single determinant, that is,

$$\langle x|z, R, P\rangle = \det\{\chi_i(\mathbf{x}_j)\} \tag{4}$$

with the spin orbitals

$$\chi_i(\mathbf{x}) = u_i(\mathbf{x}) + \sum_{j=N+1}^{K} u_j(\mathbf{x}) z_{ji}, \tag{5}$$

where $\mathbf{x}$ is the electron coordinate. In the expression for the Lagrangian, the traveling Gaussians of Eq. (3) for the nuclei are taken in the limit of zero width ($\omega \to 0$), so that the nuclei move classically. The electronic basis u_i is chosen as a set of Gaussian or contracted Gaussian-type orbitals centered on, and moving with, the average nuclear positions $\mathbf{R}$. The dynamical variables, at this level of END, are the complex, time-dependent, molecular orbital coefficients $\mathbf{z}$, and the nuclear positions $\mathbf{R}$ and the momenta $\mathbf{P}$, both of which are time-dependent.

Application of the variational principle thus provides the equations of motion for the system, which, when expressed in matrix form, are given by [15]

$$\begin{pmatrix} i\mathbf{C} & \mathbf{0} & i\mathbf{C}_\mathbf{R} & i\mathbf{C}_\mathbf{P} \\ \mathbf{0} & -i\mathbf{C}^* & -i\mathbf{C}^*_\mathbf{R} & -i\mathbf{C}^*_\mathbf{P} \\ i\mathbf{C}^\dagger_\mathbf{R} & -i\mathbf{C}^\mathbf{T}_\mathbf{R} & \mathbf{C}_{\mathbf{RR}} & -\mathbf{I}+\mathbf{C}_{\mathbf{RP}} \\ i\mathbf{C}^\dagger_\mathbf{P} & -i\mathbf{C}^\mathbf{T}_\mathbf{P} & \mathbf{I}+\mathbf{C}_{\mathbf{PR}} & \mathbf{C}_{\mathbf{PP}} \end{pmatrix} \begin{pmatrix} \dot{\mathbf{z}} \\ \dot{\mathbf{z}}^* \\ \dot{\mathbf{R}} \\ \dot{\mathbf{P}} \end{pmatrix} = \begin{pmatrix} \partial E/\partial \mathbf{z}^* \\ \partial E/\partial \mathbf{z} \\ \partial E/\partial \mathbf{R} \\ \partial E/\partial \mathbf{P} \end{pmatrix}. \tag{6}$$

The elements of the dynamical metric matrix are

$$(C_{XY})_{ik;jl} = -2\,\mathrm{Im}\frac{\partial^2 \ln S}{\partial X_{ik}\partial Y_{jl}}\bigg|_{R'=R,P'=P}, \tag{7}$$

$$\left(C_{X_{ik}}\right)_{\mathrm{ph}} = (C_X)_{\mathrm{ph};ik} = \frac{\partial^2 \ln S}{\partial z^*_{ik}\partial X_{ik}}\bigg|_{R'=R,P'=P}, \tag{8}$$

which are the nonadiabatic coupling terms, and

$$C_{\mathrm{ph};qg} = \left.\frac{\partial^2 \ln S}{\partial z^*_{\mathrm{ph}} \partial z_{qg}}\right|_{R'=R,P'=P}. \tag{9}$$

Here $S = \langle z, R', P' | z, R, P \rangle$ is the overlap between two different configurations of the system having a total energy given by

$$E = \sum_{jl} \frac{P_{jl}^2}{2M_l} + \frac{\langle z, R', P' | H_{\mathrm{el}} | z, R, P \rangle}{\langle z, R', P' | z, R, P \rangle}. \tag{10}$$

The electronic Hamiltonian, H_{el}, includes the nuclear-nuclear repulsion terms. P_{jl} denotes a Cartesian component of the momentum and M_l is the mass of nucleus l. Integration of this system of coupled differential equations yields the average position and momentum and the electronic excitation of the system as a function of time.

The details of the implementation and calculation for He^{2+} ions colliding with H, D, and T have been previously reported in Ref. [11], and thus they are not repeated here.

III. ENERGY LOSS

By solving Eq. (6), we obtain the average nuclear positions **R** and momenta **P** for projectile and target, respectively, as a function of time. In addition, the electronic wave function can be obtained from the **z** coefficients. Since the electron may be excited or captured by the projectile during the collision, it may acquire electronic momentum, which we calculate as $\mathbf{p}_e = \langle z | i\nabla | z \rangle$ for both the projectile and target. After the collision has occurred, we can calculate, with these variables, the scattering angle in the center of mass (c.m.) reference frame, the energy loss, and the occupation probability for the electrons associated with the projectile or target, which gives the probability of electron transfer, as is standard in any classical scattering treatment [16,17].

An important characteristic of the $He^{2+} \rightarrow$ H, D, and T collision system obtained in previous studies [11–13] is that for collision energies below 1 keV, the electron transfer is small, so, on average, the projectile is almost a bare charged particle. This is due to the fact that the charge-transfer cross section is small, as can be seen from the results in Fig. 1. In that figure, we compare our results with the experimental data of Havener *et al.* [18] and to the recommended cross sections by Krstić [8]. We observe a strong target isotopic effect (expanded in the inset). So the question arises whether this isotopic effect on the charge exchange influences the energy loss of the projectile.

According to classical scattering theory [16,17], in an elastic collision between a projectile of mass M_p and initial velocity v and a target at rest of mass M_b, the kinetic energy loss of the projectile will be the energy gained by the target, and is given by

$$\Delta T_n = 4\frac{\mu^2}{M_b M_p} E_0 \sin^2\left(\frac{\theta_{\mathrm{c.m.}}}{2}\right). \tag{11}$$

Here $\theta_{\mathrm{c.m.}}$ is the scattering angle in the c.m. system, and μ is the reduced mass of the system. This result is independent of the type of interaction, provided that the collision is elastic. To determine if the energy loss results for collisions of He^{2+} with H, D, and T obtained by the END approach follow Eq. (11), we show in Fig. 2 the nuclear energy loss for He^{2+} ions colliding with H, D, and T as a function of the c.m. scattering angle, as obtained by the END theoretical approach. That is, we plot $\Delta T M_b M_p/(4\mu^2 E_0)$ versus $\theta_{\mathrm{c.m.}}$. We show the results for collision energies of 50 eV/amu, and 1 and 25 keV/amu, and

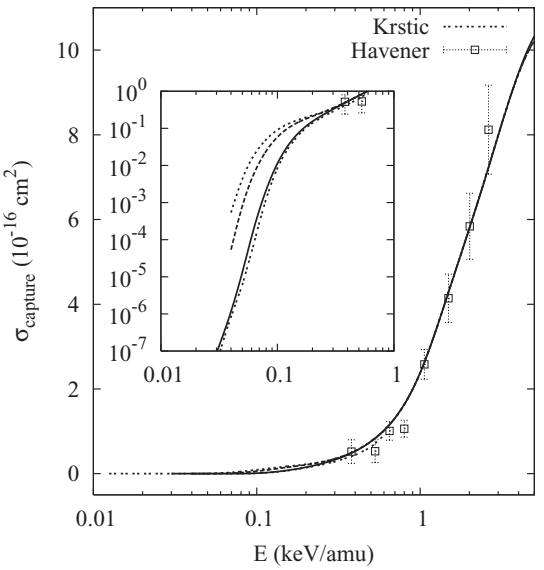

FIG. 1. Charge-transfer cross section for He^{2+} colliding with H, D, and T target atoms as a function of the projectile energy. This work: solid line, He^{2+} on H; dashed line, He^{2+} on D; dotted line, He^{2+} on T. The experimental results (□) are from Havener *et al.* [18]. The double-dotted line represents the recommended calculations from Krstić [8]. In the inset, we show the isotopic effect on the charge-transfer cross section.

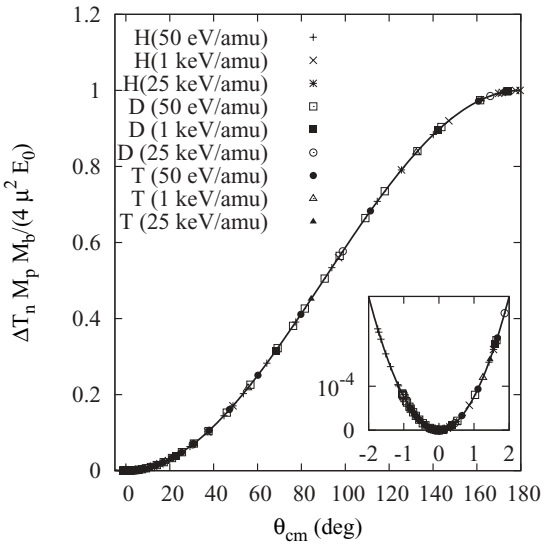

FIG. 2. Nuclear energy loss of He^{2+} colliding with H, D, and T as a function of the c.m. scattering angle, $\theta_{\mathrm{c.m.}}$, for collision energies of 50 eV/amu and 1 and 25 keV/amu. The symbols are our results from the END approach. The solid line follows from Eq. (11). In the inset, we show the small scattering angles in the c.m. where we show the negative scattering angles.

all the points agree with the classical expression (solid line). Furthermore, in the inset, we show the results for negative (attractive) scattering angles, that is, the energy loss due to the attractive part of the interaction potential, which is the result of the correct description of the collision dynamics involving the mutual interaction between the electrons and nuclei. As expected, this attractive region corresponds to small scattering angles or intermediate to large impact parameters, as we shall see later.

The scattering angle can be expressed as a function of the impact parameter in the c.m. frame as

$$\theta_{\text{c.m.}}(b, E_{0r}) = \pi - 2b \int_{r_{\min}}^{\infty} \frac{dr}{r^2 f(r)}, \tag{12}$$

where

$$f(r,b,E_{0r}) = \sqrt{1 - \frac{b^2}{r^2} - \frac{V(r)}{E_{0r}}}. \tag{13}$$

Here, $E_{0r} = \mu v^2/2$ is the energy of the projectile in the c.m. system, and $r_{\min}$ is the distance of closest approach.

For the case of a Coulomb interaction potential between two bare point charges Z_p and Z_b for projectile and target, respectively, one obtains

$$\sin\left(\frac{\theta_{\text{c.m.}}}{2}\right) = \frac{\gamma}{\sqrt{\gamma^2 + 4b^2}}, \tag{14}$$

where γ is the collision diameter defined by

$$\gamma = \frac{Z_p Z_b}{E_{0r}}. \tag{15}$$

From Eqs. (12) and (14), one notes that for the Coulombic case, the scattering angle in the c.m. is a unique function of bE_{0r}. For a screened potential, such as that of Bohr or Moliére, of the form

$$V(r) = \frac{Z_p Z_b}{r}\Phi(r), \tag{16}$$

with $\Phi(r)$ being the screening function, one sees from Eq. (12) that the Coulombic scaling rule no longer applies since Eq. (12) will not longer depend uniquely on the product bE_{0r}. This is shown in Fig. 3, where the scattering angle in the c.m. is plotted for He^{2+} ions colliding with H, D, and T as a function of bE_{0r} as obtained by END. The solid lines are the results for He^{2+} colliding with H, the dashed line is for He^{2+} colliding with D, and the dotted line is for He^{2+} colliding with T. Also, we show results from Eq. (14) for the Coulomb case (dot-dashed line). For high collision energies, our theoretical results follow a Coulombic behavior, but for low collision energies a separation from the Coulombic results appears for bE_{0r} values between 0.1 and 100. Furthermore, our theoretical data show the attractive part of the interaction while the Coulomb potential does not for low collision energies.

In Fig. 4, we show an enhancement of the attractive c.m. scattering angles as a function of bE_{0r}. We note that α particle scattering by H, D, and T does not obey a scaling law at low collision energies, as would be the case for a Coulomb interaction involving a bare projectile colliding with a bare

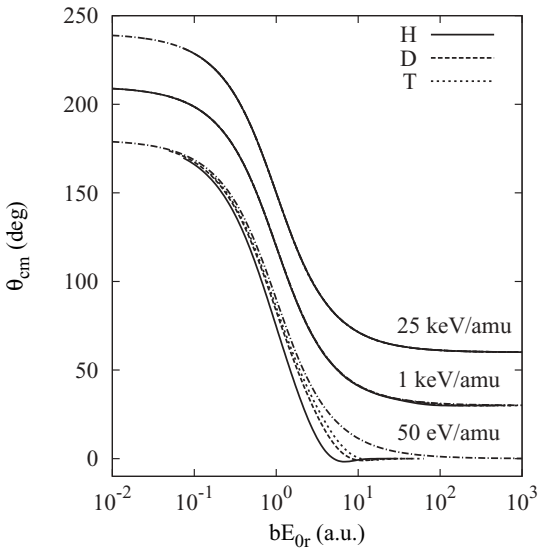

FIG. 3. Scattering angle in the c.m. as a function of bE_{0r} for He^{2+} colliding with H, D, and T for 50 eV/amu and 1 and 25 keV/amu as obtained with END. Solid line: He^{2+} on H; dashed line: He^{2+} on D; dotted line; He^{2+} on T. Coulombic results [Eq. (14)]: dot-dashed line. Note that the results for 1 and 25 keV/amu are shifted upward by 30° on the y axis for clarity.

nuclear target [Eq. (14)]. The impact parameter region where discrepancies occur involves intermediate to large impact parameters for which screening of the target is important. In the same figure, we show the results of using an interaction potential obtained by means of a screened frozen charge distribution for a target atom in its $1s$ state interacting with a

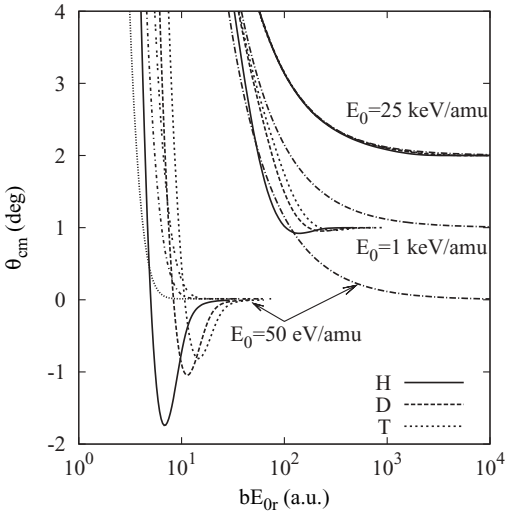

FIG. 4. Detail of Fig. 3 showing the small scattering angles for the attractive and repulsive parts of the interaction. Also we show the results of the screened frozen charge distribution potential for He^{2+} with H (short-dot line), He^{2+} with D (dot-short dash line), and He^{2+} with T (double-dot line) for the collision energy of 50 eV/amu. Note the Coulomb scattering angle departure for the results at 50 eV/amu (signaled by arrows). For clarity, the data for 1 and 25 keV/amu are shifted upward by 1° on the the y axis.

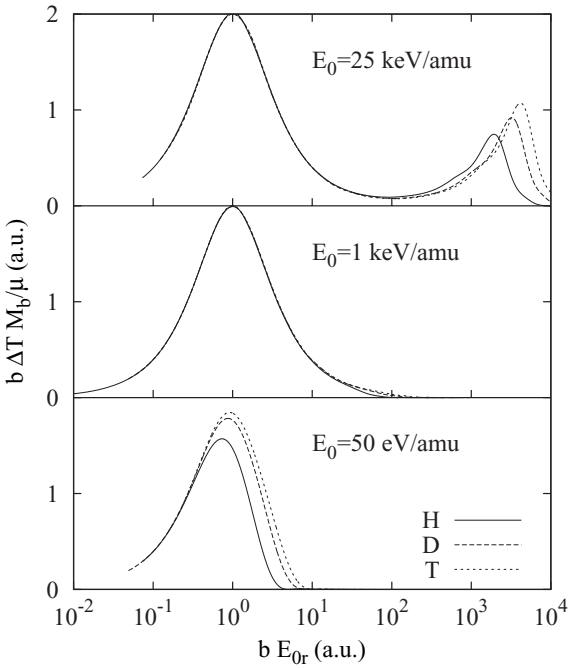

FIG. 5. Total energy loss for He^{2+} colliding with H, D, and T as a function of bE_{0r} for projectile energies of 50 eV/amu and 1 and 25 keV/amu.

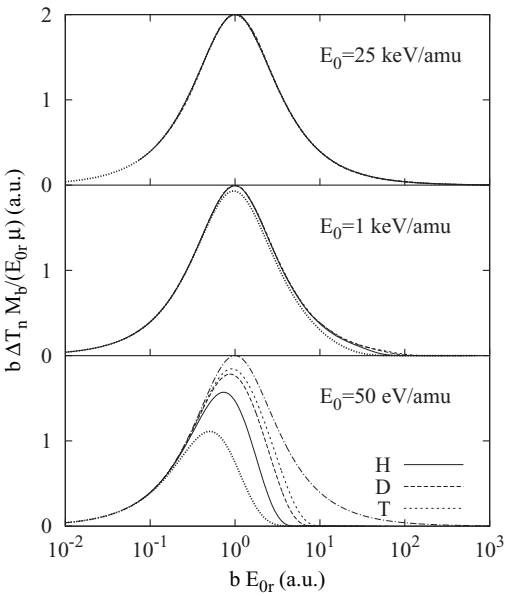

FIG. 6. Nuclear energy loss for He^{2+} ions colliding with H, D, and T as a function of bE_{0r}. The short dotted line follows from our calculations using a screened model potential. The dot-dashed line represents the results of Eq. (17) using a Coulomb potential.

bare projectile with nuclear charge $Z_p = 2$ (see the Appendix). This potential produces results that are in closer agreement with our theoretical data than those obtained from the Coulomb potential. However, this screened potential lacks a proper description of the attractive region of the interaction. The difference in the scattering angles (and, thus, in the trajectory) can be several degrees at low collision energies when obtained by a Coulombic, a screened, and an *ab initio* treatment.

We now turn to the dependence of the energy loss on the impact parameter b. For the case of a Coulombic potential, the energy gain by the target is obtained by substituting Eq. (14) into Eq. (11):

$$\Delta T_n = \frac{2Z_p^2 Z_b^2}{M_b v^2} \frac{1}{b^2 + \left(\frac{\gamma}{2}\right)^2}. \tag{17}$$

Thus, we note that for the Coulombic case, the nuclear energy loss times the impact parameter is a unique function of bE_{0r}.

In Fig. 5, we show the total (electronic plus nuclear) scaled energy loss $b\Delta T M_b/\mu$ for the projectile when it collides with H, D, and T as a function of bE_{0r} for 50 eV/amu and 1 and 25 keV/amu obtained by our END approach. We note two characteristic peaks, one around $bE_{0r} \sim 1$ that corresponds to the nuclear energy loss, and a second peak that appears only in the high energy and high impact parameter region, which represents the electronic energy loss, as we shall see later. For the moment, we concentrate on the first peak representing the nuclear stopping power.

From Eq. (17), we recall that $b\Delta T M_b/\mu$ is a function of bE_{0r}. In Fig. 6, we show our theoretical results for the nuclear energy loss of He^{2+} ions colliding with H, D, and T as a function of bE_{0r} for 50 eV/amu and 1 and 25 keV/amu, as obtained using END. In that figure, we compare with the Coulombic results [Eq. (17)] (dot-dashed line) and those obtained by the screened potential (see the Appendix). The results at high energies perfectly follow the calculation using a Coulomb potential, however the low-energy collision does not. Furthermore, there are differences in the H, D, and T contribution in the low collision energy region as a function of bE_{0r}. This is seemingly due to the charge-transfer isotope effect. Even the frozen charge potential results differ significantly, when for the scattering angle they gave a better description than the Coulombic potential, as shown in Fig. 4.

Now, we return to the second peak. In Fig. 7, we show the electronic energy loss, obtained by subtracting the nuclear energy loss from the total energy loss, as a function of b for He^{2+} ions colliding with H, D, and T targets at collision energies of 50 eV/amu and 1 and 25 keV/amu. We note that there is no scaling law for the electronic energy loss as a function of bE_{0r} (see Fig. 5), but it exhibits deviations between the results of the target atoms H, D, and T. These deviations disappear when plotted as a function of E_0 in the high-energy region, as shown in Fig. 7. At intermediate energies (b) of 1 keV/amu, one notes the effect of the Stueckelberg oscillations in the electron capture cross section reflected in the electronic energy loss in the intermediate impact parameter region, thus showing an isotopic effect, although not as pronounced as in the electron capture cross section. Note that the results have been scaled by a factor of 40. For low collision energies (*c*), the Stueckelberg oscillations disappear but their effect in the projectile charge is observed in the electronic energy loss. Note the scaling factor of 10^4 in the plotted data, so the electronic energy loss at these energies is too small.

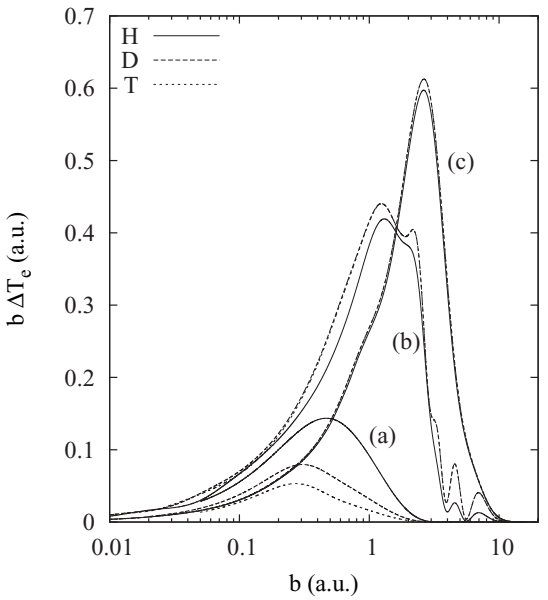

FIG. 7. Electronic energy loss for He^{2+} ions incident with H, D, and T as a function of b. The lines are labeled as in Fig. 6. Line (a) corresponds to a collision energy of 50 eV/amu and is scaled by a factor of 10^4; line (b) corresponds to 1 keV/amu and is scaled by a factor of 40; and line (c) corresponds to 25 keV/amu and no scaling factor.

A. Validity of classical trajectories

Since all these previous results follow from the properties of the nuclei trajectories obtained from the solution of the time-dependent Schödinger equation by the END method, the question arises as to what is the region of applicability of a classical trajectory in terms of the collision energy and impact parameter. This question was already addressed by Bohr in his classic work of 1948 [16] (Sec. 1.3; see also Ref. [1]) and by Williams [19].

For a classic treatment to hold, two conditions must be satisfied:

(1) The orbit of the particles must be well defined in relation to their distance [19].

(2) The deflection due to the collision must also be well defined.

If a is the range or extension of the potential (scattering length), then the first condition requires $M_p v a \gg \hbar$, that is, the wavelength should be small compared with the dimensions of the scatterer. The second condition leads us to "Bohr's kappa larger than 1" criteria, that is

$$\kappa = \frac{2|Z_1 Z_2|}{v} > 1, \tag{18}$$

which can also be stated as $\lambda/\gamma < 1$, where λ is the de Broglie wavelength of the projectile and γ is the collision diameter given by Eq. (15). This result follows from the fact that to avoid quantum effects and the minimization of the spreading of the incoming wave packet, the projectile nuclei wavelength must be smaller than the collision diameter. Thus, the validity of a classical treatment is in the region

$$\frac{1}{M_p a} \ll v < 2|Z_1 Z_2|. \tag{19}$$

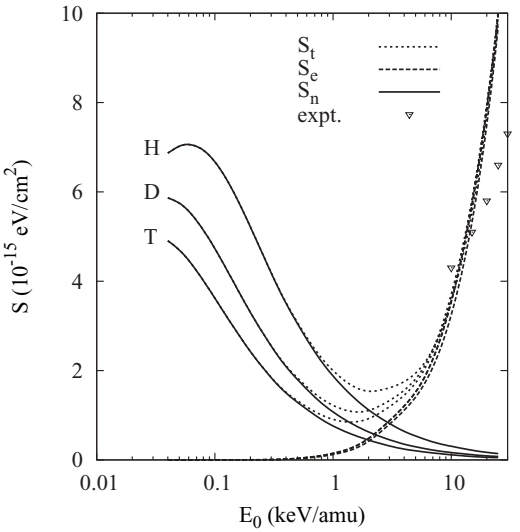

FIG. 8. Total stopping power for He^{2+} colliding with H, D, and T as a function of the incident projectile energy obtained is this work. The experimental data ($\triangledown$) are from Ref. [20].

In our case, for instance, if the scattering length is of the order of the atom size $\sim a_0 \sim 1$ a.u., we have that our results are valid for projectile velocities $0.001 \ll v \ll 4.0$ a.u. (or 10 meV/amu $\ll E_0 \ll$ 400 keV/amu). Hence, we believe that it is justified to use classical trajectories within the energy range studied in this work.

IV. STOPPING CROSS SECTION

From Eq. (1), the stopping cross section is given by the integral of the energy loss over the impact parameter region, which can be written as

$$S_i(E_0) = 2\pi \int_0^\infty b \Delta T_i(b, E_0)\, db, \tag{20}$$

where i stands for the total, electronic, or nuclear contribution.

In Fig. 8, we show the stopping cross section as obtained from END for He^{2+} ions incident on H, D, and T as a function of the initial projectile energy E_0 for a collision energy range from 30 eV/amu up to 25 keV/amu. In this figure, we show the nuclear as well as the electronic contributions to the stopping cross section and compare to the experimental data of Ref. [20]. In our case, the single channel He^{2+} has a large stopping cross section in the high collision energy region for the electronic contribution to the stopping cross section. Also, we note a threshold in the electronic stopping cross section. This threshold is the result of the minimum energy transferred by the projectile to the target to produce an electronic excitation from $n = 1$ to 2 in the hydrogen target. In Ref. [21], we report that the minimum projectile energy to produce such an excitation is when $E_0 > M_p(E_2 - E_1)/4m_e$, where E_i are the energy levels in the hydrogen atom. In our case, we obtain that $E_0 > 0.7$ keV/amu, in complete agreement with our results shown in Fig. 8.

If we assume a Coulombic interaction, we obtain an analytical expression for the nuclear stopping power by

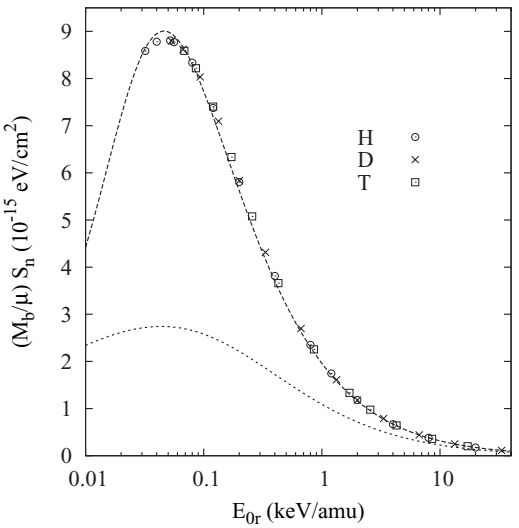

FIG. 9. Scaled total stopping power for He^{2+} colliding with H, D, and T as a function of the projectile energy. The symbols are our END results. The long dashed line is Eq. (21). The short dashed line corresponds to the ZBL results of Eq. (22).

substituting Eq. (17) into Eq. (20):

$$S_n = \frac{\mu}{M_b}\frac{\pi Z_p^2 Z_b^2}{E_{0r}} \ln\left[1 + \left(\frac{2E_{0r}b_{\max}}{Z_p Z_b}\right)^2\right], \qquad (21)$$

where we have used an upper limit, $b_{\max}$, in the impact parameter due to the long range of the Coulomb potential. Bohr analyzed this problem [1,16] and found that a proper cutoff would be $b_{\max} \sim v/w_0$, where w_0 is the characteristic frequency of the electron harmonically bound to the target. However this assumption is valid for $v \gg v_0$ with v_0 the Bohr velocity. For low velocities, we will assume $b_{\max}$ constant and determine its values from the *ab initio* data by means of a fitting procedure. With this assumption, a characteristic of Eq. (21) is that $S_n M_b/\mu$ is a unique function of E_{0r}, recalling that it assumes a bare projectile with charge Z_p.

In Fig. 9, we show the scaled END nuclear cross sections for He^{2+} ions colliding with H, D, and T as a function of E_{0r}. In this figure, we show the analytical results of Eq. (21) and see an excellent agreement for this particular system. In this case, we find that $b_{\max} = 1.17$ a.u. as the maximum impact parameter required in a Coulomb scattering. This result is in agreement with the largest impact parameter for electron capture for this system, as can be seen in Refs. [11–13], where the largest electron capture probability occurs for $b < 1.5$ a.u. Thus, we confirmed the scaling law for the nuclear stopping cross section for a projectile colliding with targets differing only in mass. Also, in Fig. 9 we present the results of Ziegler, Biersack and Littmark (ZBL) [3] (see Eq. (2)–72), which can be rewritten as a unique function of E_{0r} and that we present here for completeness,

$$S_n(E_{0r}) = \frac{\mu}{M_b}\frac{8.462 Z_p Z_b}{\left(Z_p^{0.23} + Z_b^{0.23}\right)}\bar{S}_n(\epsilon) \qquad (22)$$

with

$$\epsilon = \frac{32.53 E_{0r}}{Z_p Z_p\left(Z_p^{0.23} + Z_b^{0.23}\right)}$$

and

$$\bar{S}_n(\epsilon) = \frac{\ln(1 + 1.1383\epsilon)}{2(\epsilon + 0.01321\epsilon^{0.21226} + 0.19593\epsilon^{0.5})}$$

for $\epsilon < 30$, and $S_n(E_0)$ is given in units of 10^{-15} eV cm^2/at. The first thing to note is that the ZBL expression and Eq. (21) behave as $\ln(E_{0r})/E_{0r}$ at large collision energies. However, at low collision energies, our expression is quadratic on the energy in the logarithmic term when ZBL depends linearly in E_{0r} in the logarithmic term. Another characteristic of ZBL is that the scaling length $a = a_0/(Z_p^\gamma + Z_b^\gamma)$ with $\gamma = 0.23$ appears in the expression, which arises from the interaction of neutral atoms (both projectile and target), so it is unsuitable for ionic interactions. This is observed in Fig. 9, which shows the ZBL contribution is small compared to our END results. So care must be taken when comparing the nuclear stopping cross section for ionic systems where the electron capture cross section is small, to those where neutral atom interactions are assumed, as in the ZBL formula.

V. CONCLUSIONS

The energy loss of a projectile, when it collides with an atomic target, requires a proper description of the interaction potential. Due to dynamic processes such as charge transfer, that interaction is not universal but depends on the region of interaction and on the target mass. However, many of the energy loss processes such as scattering in the c.m. frame can exhibit a universal behavior described by a scaling law. In this work, we have shown that such a scaling law for the scattering and energy loss of He^{2+} ions colliding with H, D, and T exists in the low to intermediate energy region. We find that the scattering in the c.m. frame shows such universal behavior, which is a result of momentum and mass conservation, independent of the type of interaction. Due to charge exchange, the energy loss departs from a scaling law, except for high-energy collisions, which follow a Coulomb-type interaction more closely. Finally, we show that the nuclear energy loss is independent of the details of the interaction and shows a scaling law for the target atomic mass as a function of bE_{0r}. Thus, for this system, there is no influence of the charge exchange isotope effect of the target in the nuclear stopping cross section of the projectile. In the electronic energy loss, such an isotopic effect is present through Stueckelberg oscillations, but its contribution is small. Also, the electronic stopping cross section shows a threshold in the projectile energy due to the minimum momentum transfer necessary by the projectile to produce an electronic excitation in the target. Finally, the nuclear stopping cross section has a universal behavior as a function of E_{0r}. Thus, in conclusion, care must be taken when comparing ionic systems stopping cross sections results to those of neutral systems, as assumed, for example, by the ZBL model. All these results are based on classical trajectories that are valid for meV/amu $\ll E_p \ll$ 400 keV.

ACKNOWLEDGMENTS

R.C.T. acknowledges support from PAPIIT-UNAM 107-108 as well as fruitful and enjoyable discussions with Salvador Cruz on this work.

APPENDIX: MODEL POTENTIAL FOR THE PROJECTILE-TARGET INTERACTION

Since the electron capture cross section is small, we assume that the target charge distribution is not modified by the collision. For a hydrogen target with a wave function given by $\psi(\mathbf{r}) = \sqrt{1/4\pi}e^{-r}$, the potential produced by the electronic plus nuclear charge at a point $\mathbf{r}$ when interacting with a bare charge Z_p is

$$V(\mathbf{r}) = \frac{Z_p}{r} - Z_p \int \frac{\rho(\mathbf{r}')}{|\mathbf{r} - \mathbf{r}'|} d\mathbf{r}', \tag{A1}$$

where $\rho(\mathbf{r}) = \psi(\mathbf{r})^* \psi(\mathbf{r})$. Thus one obtains

$$V(r) = \frac{Z_p}{r} e^{-2r}(1 + r). \tag{A2}$$

This potential does not include polarization effects as the projectile gets closer to the target, and thus is completely repulsive for all distances. For small distances, where $Z_b r \ll 1$, the projectile sees a Coulombic potential. For intermediate to large distances, the projectile feels a screened Yukawa-type potential that falls off faster than a Coulombic potential.

[1] E. Bonderup, *Penetration of Charged Particles Through Matter* (Institute of Physics, University of Århus, Denmark, 1981).

[2] N. Bohr, Phil. Mag. **25**, 10 (1913).

[3] J. F. Ziegler, J. P. Biersack, and U. Littmark, *The Stopping and Range of Ions in Solids* (Pergamon, New York, 1985). For a thorough description of the most recent version of this program, see [http://www.srim.org].

[4] V. A. Krasnopolsky, M. J. Mumma, M. Abbott, B. C. Flynn, K. J. Meech, D. K. Yeomans, P. Feldman, and C. Cosmovici, Science **277**, 1488 (1997).

[5] D. Bodewits, Z. Juhász, R. Hoekstra, and A. G. G. M. Tielens, Astrophys. J. Lett. **606**, L81 (2000).

[6] D. Bodewits, R. Hoekstra, B. Seredyuk, R. W. McCullough, G. H. Jones, and A. G. G. M. Tielens, Astrophys. J. **642**, 593 (2006).

[7] Y. Matsuzaki, H. Date, K. L. Sutherland, and Y. Kiyanagi, Radiol. Phys. Technol. **3**, 84 (2010).

[8] P. S. Krstić, J. Phys. B **37**, L217 (2004).

[9] T. Minami, T. G. Lee, M. S. Pinzola, and D. R. Schultz, J. Phys. B **41**, 135201 (2008).

[10] A. T. Le, C. D. Lin, L. F. Errea, L. Méndez, A. Riera, and B. Pons, Phys. Rev. A **69**, 062703 (2004).

[11] N. Stolterfoht, R. Cabrera-Trujillo, P. S. Krstić, Y. Öhrn, E. Deumens, and J. R. Sabin, Int. J. Quantum Chem. **109**, 3063 (2009).

[12] N. Stolterfoht, R. Cabrera-Trujillo, Y. Öhrn, E. Deumens, R. Hoekstra, and J. R. Sabin, Phys. Rev. Lett. **99**, 103201 (2007).

[13] N. Stolterfoht, R. Cabrera-Trujillo, P. S. Krstić, R. Hoekstra, Y. Ohrn, E. Deumens, and J. R. Sabin, Phys. Rev. A **81**, 052704 (2010).

[14] B. H. Bransden and M. R. C. McDowell, *Charge Exchange and the Theory of Ion-Atom Collisions* (Clarendon, New York, 1992).

[15] E. Deumens, A. Diz, R. Longo, and Y. Öhrn, Rev. Mod. Phys. **66**, 917 (1994).

[16] N. Bohr, Mat. Fys. Medd. K. Dan. Vidensk. Selsk. **18**, no. 8 (1948).

[17] H. Goldstein, *Classical Mechanics*, 2nd ed. (Addison-Wesley, Reading, MA, 1980).

[18] C. C. Havener, R. Rejoub, P. S. Krstić, and A. C. H. Smith, Phys. Rev. A **71**, 042707 (2005).

[19] E. J. Williams, Rev. Mod. Phys. **17**, 217 (1945).

[20] J. Cuevas, M. Garcia-Munoz, P. Torres, and S. K. Allison, Phys. Rev. **135**, A335 (1964).

[21] R. Cabrera-Trujillo, J. R. Sabin, Y. Öhrn, and E. Deumens, Phys. Rev. Lett. **84**, 5300 (2000).